Bimetallic hexanuclear clusters in Ce/Zr-UiO-66 MOFs: In situFTIR spectroscopy and modelling insights

Bimetallic hexanuclear clusters in Ce/Zr-UiO-66 MOFs: *in situ* FTIR spectroscopy and modelling insights†

Cesare Atzori*,[a] Kirill A. Lomachenko,[b] Jannick Jacobsen,[c] Norbert Stock,[c] Alessandro Damin,[a] Francesca Bonino,[a] Silvia Bordiga[a]

† *Deeply indebted to Carlo Lamberti, who inspired this work.*

***In situ* FTIR spectroscopy in combination with results from DFT calculations was used to determine the composition of mixed-metal clusters $\{Ce_xZr_{6-x}(\mu_3\text{-}O)_4(\mu_3\text{-}OH)_4\}$ in Ce/Zr-UiO-66 compounds. Detailed, quantitative evaluation of vibrational bands ν(OH) of $(\mu_3\text{-}OH)Ce_xZr_{3-x}$ groups allowed us to distinguish between two possible models: a solid solution or the presence of distinct clusters. This relatively straightfoward method should be also transferable to other mixed-metal metal-organic frameworks (MOFs).**

Mixed-metal MOFs were recently introduced in the literature as promising materials for functional applications like heterogeneous catalysis or gas storage and separation.[1–3] Bimetallic Ce/Zr-UiO-66 with the composition $[Ce_xZr_{6-x}(\mu_3\text{-}O)_4(\mu_3\text{-}OH)_4(BDC)_6]$ with $0<x<6$, BDC^{2-} = 1,4-benzenedicarboxylate, among others, caught interest in the literature as a redox catalyst.[4,5] Many authors explored recently the catalytic possibilities offered by Ce based MOFs, such as in the aerobic oxidation of benzylic alcohol,[6] the selective catalytic reduction (SCR) of nitrogen oxides[7] or the oxidation of styrene to its epoxide.[8]

Structural information about MOFs is usually obtained from diffractometric studies with X-rays or neutrons. Thus, only the average periodic arrangement but no local features like defects,[9–11] metal[12] or linker[13] substitution or post-synthetic functionalizations can be detected.[14] To address this challenge local spectroscopic techniques like IR/Raman,[10,11,15] XAS,[16,17] EPR[18] or SSNMR[19] have been carried out.

Recently a multi-edge XAS study showed that Ce/Zr-UiO-66 compounds are truly bimetallic and exhibit a strong preference to form, instead of a solid solution, predominantly three clusters: Ce_6, $CeZr_5$ and Zr_6.[17] The relative cluster concentration as a function of the Ce content in Ce/Zr-UiO-66 compounds is represented in Figure 1a (details are reported in the SI, Section 1) for Three Cluster Model (**TCM**), as described by Lomachenko et al.[17] This model is characterised by the predominant formation of bimetallic $CeZr_5$ cornerstones which coexist either with pure Zr_6 or with pure Ce_6 clusters at Ce content below or above 16.7% (i.e. 1/6), respectively, adding up to the overall concentration of Ce in the material. On the other hand, for a solid solution a Multi Cluster Model (**MCM**), consisting in a mixture of all seven possible Ce_xZr_{6-x} clusters, is expected as shown in Figure 1b (details in Section 2 of the SI).

In the present paper we propose an innovative metodology, based on FTIR spectroscopy coupled with DFT calculations, to determine the composition of the M-O cluster structures in mixed-metal Ce/Zr-UiO-66 compounds.

The synthesis of the pure Ce-UiO-66 and Zr-UiO-66 samples and the mixed-metal Ce/Zr-UiO-66 compounds was accomplished following published synthesis procedures.[3,4,17,20] The detailed synthetic procedures are reported in the SI (Section 3). The mixed-metal samples will be referred to as CeXX in the following, XX being the fraction of Ce in the total metal content (in mol %) determined by EDX (SI, section 4).[5,17]

IR spectra of the eight materials used in this study are characterized by the presence of sharp ν(OH) bands due to the four μ_3-OH groups in each hexanuclear metal cluster (Figure 2).[21] These vibrational bands are known to shift considerably depending on the metal cations present in the M-O cluster, as it occurs for pure Hf, Zr, Ce and Th isostructural UiO-66 MOF materials. [22] In the case of mixed-metal UiO-66 compounds**,** it should not be surprising to observe bands at different wavenumbers from those ones reported for pure Zr and Ce materials as each OH group is actually bridging three metal cations. Four different cases can be expected, by considering μ_3-OH as a bridge among i) 3 Ce ii) 2 Ce and 1 Zr iii) 1 Ce and 2 Zr iv) 3 Zr (see Figure 2a). In order to calculate the relative abundance of these species in a perfect solid solution case (**MCM**) as a function of the total Ce content, a combinatorial approach was applied (details in Section 2, SI) firstly to the hexanuclear clusters Ce_xZr_{6-x} (Figure 1b) and then to the μ_3-OH groups (Figure 1d). Details are presented in the SI (Section 5). The same calculations were also applied to the **TCM** model (containing exclusively Ce_6, $CeZr_5$ and Zr_6 clusters) giving speciation diagrams for metal clusters and μ_3-OHs in Figures 1a and 1c respectively.

[a] *Department of Chemistry, NIS and INSTM Reference Centre, Università di Torino, Via G. Quarello 15, I-10135 and Via P. Giuria 7, I-10125 Torino, Italy.*
[b] *European Synchrotron Radiation Facility, 71 Avenue des Martyrs, CS 40220, 38043 Grenoble Cedex 9, France.*
[c] *Institut für Anorganische Chemie, Christian-Albrechts-Universität zu Kiel, Max-Eyth-Straße 2, 24118 Kiel, Germany.*

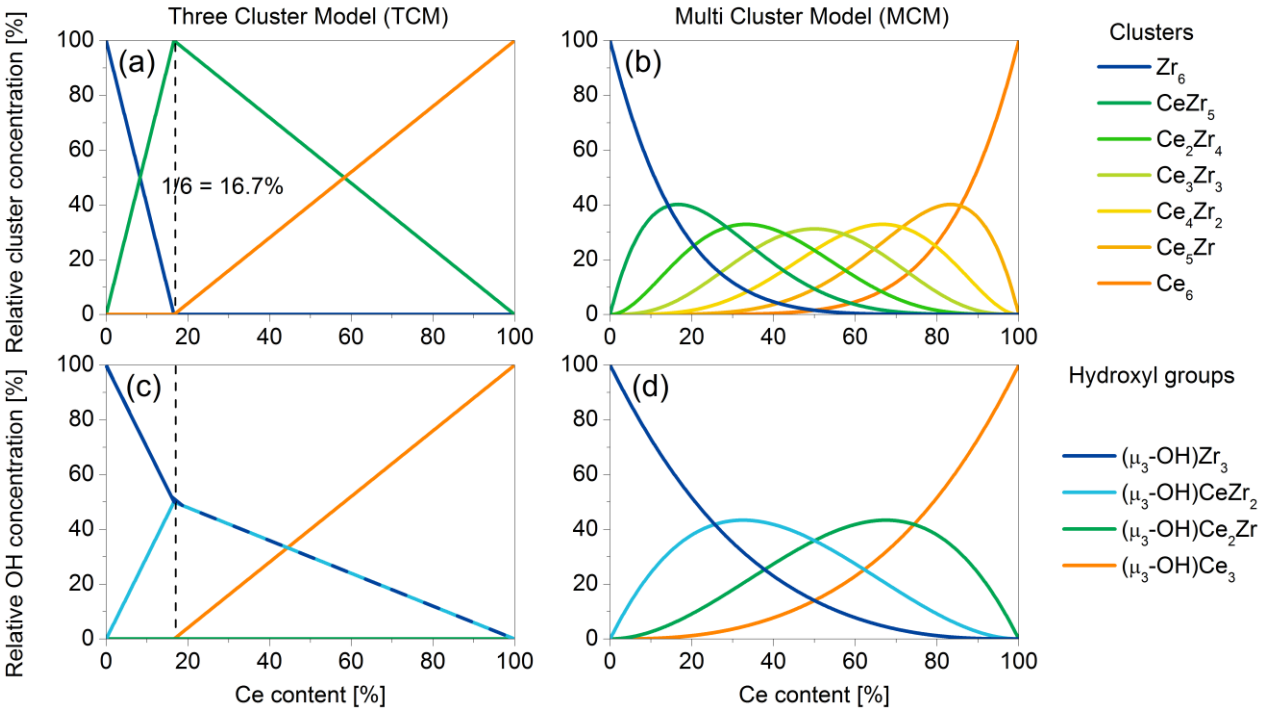

Figure 1 - Calculated cluster composition of Ce/Zr-UiO-66 materials vs. the total Ce content (percentage) under the TCM (a) and the MCM (b). The relative (μ_3-OH) concentration (in terms of the connecting Ce or Zr atoms) have been calculated following the TCM (c) or MCM (d).

Comparing the cluster compositions in the two models (Figures 1a and 1b), apart from the obvious absence of any mixed-metal cluster except for $CeZr_5$, the concentration of Zr_6 clusters diminishes with a qualitatively similar rate upon Ce addition, while Ce_6 cluster concentration is lower in **MCM** compared to **TCM** for intermediate loadings. The relative concentrations of the calculated (μ_3-OH)Ce_xZr_{3-x} species follow a similar trend in the two models, with the difference of (μ_3-OH)Ce_2Zr species thatare only present in the **MCM** (Figures 1b and 1d). This is due to the fact that each $CeZr_5$ cluster, having four μ_3-OH groups, presents only two different types of μ_3-OH groups: those linked to 1 Ce and 2 Zr or 3 Zr. The relative abundance of these two species is 1:1 (two OH moieties of each type).

This relative simplicity suggested us to exploit computational chemistry to simulate the vibrational bands of these species. Four different periodic models (Zr_6, $CeZr_5$ Ce_3Zr_3 and Ce_6), starting from the crystallographic information concerning Zr-UiO-66,[23] Ce-UiO-66[4] and the cell parameters obtained from mixed Ce/Zr materials by Lammert et al.[20] were built and optimized with the CRYSTAL17[24] code and using the B3LYP exchange-correlation functional (details are reported in Section 6 of the SI). The simulated IR bands of the ν(OH) stretching modes resulting from these calculations (Figure 2a), show, as expected,[25] sharp signals for both (μ_3-OH)Zr_3 and (μ_3-OH)Ce_3 species (respectively at 3674 cm^{-1} and 3648 cm^{-1}) and, in between, one band for the (μ_3-OH)$CeZr_2$ case at 3667 cm^{-1} and at 3658 cm^{-1} for the (μ_3-OH)Ce_2Zr species.

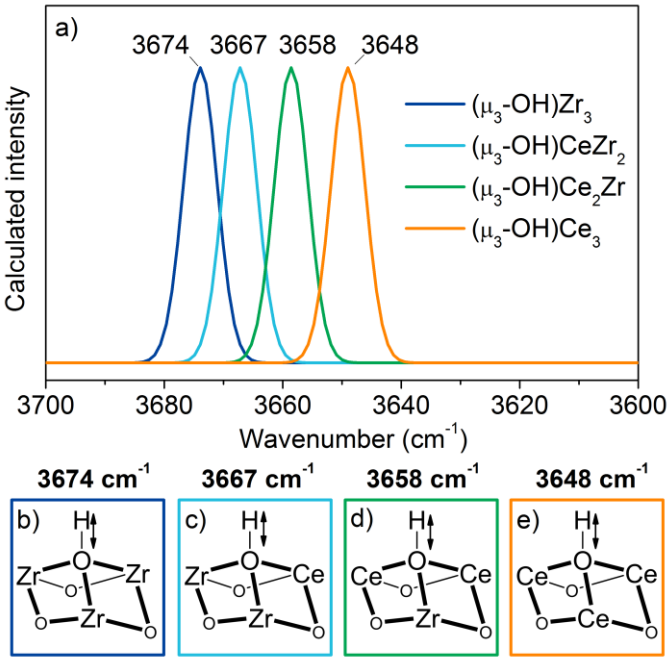

Figure 2 - Calculated IR spectra of the ν(OH) bands of (μ_3-OH) bridging three Zr (blue curve), one Ce and two Zr (green curve), two Ce and one Zr (cyan curve) and three Ce (orange curve). Atomistic models of the described situations are reported, respectively, in insets b, c, d and e.

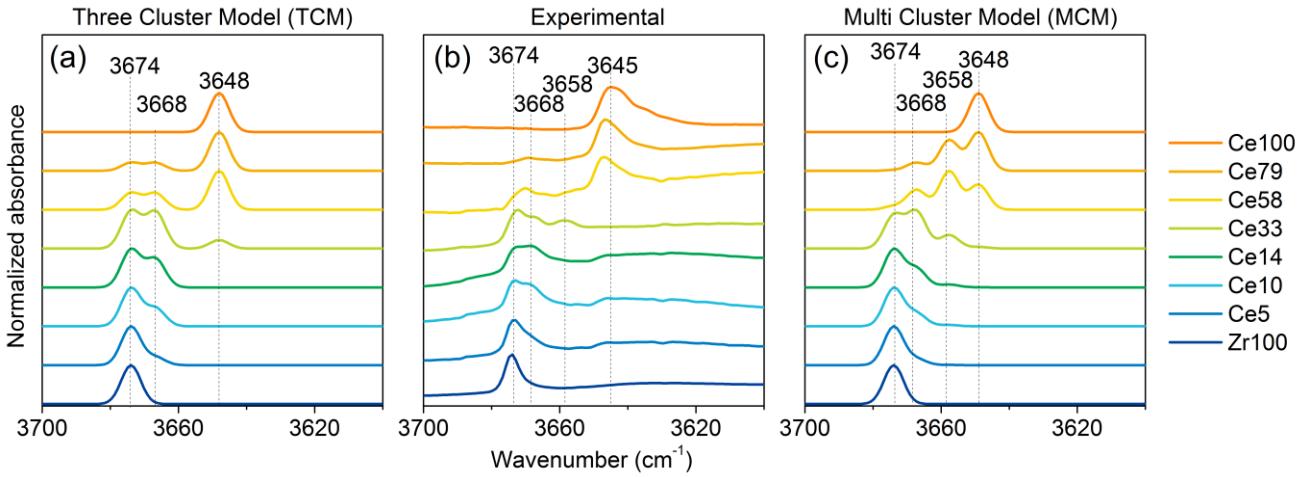

Figure 3 – Comparison between the experimental (b) and the calculated IR spectra ν(OH) region of all Ce/Zr-UiO-66 samples under the TCM (a) or MCM (c). Every spectrum is normalized to unitary value at the maximum absorbance.

Measured IR spectra obtained after thermal activation (details are reported in the SI, Table S7) for the whole set of samples used in this work are shown in Figure 3b. The spectra contain a set of sharp bands in the region between 3700-3600 cm^{-1}, ascribable to ν(OH) stretching modes. Starting from the full-Zr sample (Zr100) only one sharp band at 3674 cm^{-1} is observed in accordance to literature[3,21,26] and to our DFT calculations (Figure 2a) which is assigned to the μ_3-OH groups from the hexanuclear clusters. Comparing this spectrum with the one obtained on the other samples containing increasing amounts of Ce, a new band at 3668 cm^{-1} is observed whose intensity is increasing with the Ce concentration from the Ce5 to the Ce14 sample. This band can be assigned to ν(OH) stretching modes of (μ_3-OH)$CeZr_2$ as shown by our DFT calculations (Figure 2a). The weak band at 3658 cm^{-1} present in the Ce33 sample in addition to the other two may be ascribed to (μ_3-OH)Ce_2Zr species in Ce_xZr_{6-x} clusters with x > 1. The samples at higher Ce concentration, Ce66 and Ce79, show a new band at 3645 cm^{-1}, readily ascribable to (μ_3-OH)Ce_3 species as evidenced by our simulations and by Islamoglu et al.,[25] besides the doublet at 3674 and 3668 cm^{-1}. Finally, the pure Ce100 sample exhibits only one band at 3645 cm^{-1}.

IR-spectra presented for **TCM** and **MCM** in Figure 3a and 3d, respectively, were calculated by making linear combinations of the bands reported in Figure 2a and using the relative abundances of (μ_3-OH)Ce_xZr_{3-x} species as coefficients (Table S6). Details are given in the SI, Sections 5 and 8. Another approach that could be used in these calculations would be to make linear combinations of the calculated spectra instead of the bands; however because of the complexity of the MCM it would require a calculation of the spectra for every Ce_xZr_{6-x} case, increasing dramatically the computational cost. These linear combinations (see details in Section 8 of the SI) describe a physical situation in the approximation of an equal molar extinction coefficient among all ν(OH) bands, as the relative intensity of the vibrational bands is linearly dependent to the concentration of these species in the sample. This approximation is validated by looking at the spectra calculated from the Ce_6, $CeZr_5$ and Zr_6 crystalline models (Figure S1).

Comparing Figure 3b with 3a and 3c, an excellent agreement between the experimental and the simulated spectra of **TCM** is observed. In particular, it can be appreciated by comparing the **TCM** and **MCM** performance for Ce79 and Ce58 samples, where the difference between the two models is the highest. At the same time, a small peak at 3658 cm^{-1}, observable in the experimental spectrum of Ce33 sample, indicates that a small fraction of cornerstones different from $CeZr_5$ and Ce_6 (and therefore, not present in the TCM model) can also be formed at the intermediate Ce content.

A second possibility to get detailed information on the cluster composition using FTIR spectroscopy is the use of probe molecules.[27] The Lewis-acidity of the materials depends on metal composition and CD_3CN can be employed as probe molecule (see Section 10, SI). This molecule was chosen for its ability to deform the coordination sphere of the metal centres[27,28] and shows interactions even in the absence of an open-metal site like for UiO-66. It confirms the availability of both Ce^{4+} and Zr^{4+} for interaction with guest species. However, it does not provide any additional structural insight on the hexanuclear Ce_xZr_{6-x} cluster structure.

The reasoning of the preferential formation of defined cluster stoichiometries among all the possible one may found a thermodynamic or a kinetic way of explanation. While the first one was already studied by DFT calculations[17], highlighting not any higher stability for peculiar cluster compositions, the latter kinetic explanation (due to the complex and still mostly unknown synthesis mechanism) should be preferred.

Material defectivity, vastly found in UiO-66 materials, may play a role in selecting which cluster compositions are preferred and may be considered as another tool in engineering mixed-metal MOFs.

Concluding, the application of vibrational spectroscopy coupled with computational simulation can be applied to get detailed information on mixed-metal MOFs. Thus for six mixed-metal Ce/Zr-UiO-66 compounds the presence of three distinct clusters (**TCM**) as main constituents was confirmed. Additionally and complementarily to the results from EXAFS spectroscopy (which is a powerful averaging technique in determining abundant moieties, but may miss minority species), the observation of (μ_3-OH)Ce_2Zr species demonstrates the presence of a small concentration of mixed-metal Ce_xZr_{6-x} clusters (x = 2-5) at intermediate Ce contents.

Notes and references

There are no conflicts to declare.

The simulations were performed on resources provided by UNINETT Sigma2, the National Infrastructure for High Performance Computing and Data Storage in Norway, under project number NN9381K.

1 M. Y. Masoomi, A. Morsali, A. Dhakshinamoorthy and H. Garcia, *Angew. Chemie - Int. Ed.*, 2019, **58**, 15188–15205.

2 S. Abednatanzi, P. Gohari Derakhshandeh, H. Depauw, F. X. Coudert, H. Vrielinck, P. Van Der Voort and K. Leus, *Chem. Soc. Rev.*, 2019, **48**, 2535–2565.

3 J. H. Cavka, S. Jakobsen, U. Olsbye, N. Guillou, C. Lamberti, S. Bordiga and K. P. Lillerud, 2008, **6**, 13850–13851.

4 M. Lammert, M. T. Wharmby, S. Smolders, B. Bueken, A. Lieb, K. A. Lomachenko, D. De Vos and N. Stock, *Chem. Commun.*, 2015, **51**, 12578–12581.

5 M. Lammert, C. Glißmann and N. Stock, *Dalt. Trans.*, 2017, **46**, 2425–2429.

6 S. Smolders, A. Struyf, H. Reinsch, B. Bueken, T. Rhauderwiek, L. Mintrop, P. Kurz, N. Stock and D. E. De Vos, *Chem. Commun.*, 2018, **54**, 876–879.

7 S. Smolders, J. Jacobsen, N. Stock and D. De Vos, *Catal. Sci. Technol.*, 2020, **10**, 337–341.

8 R. Dalapati, B. Sakthivel, A. Dhakshinamoorthy, A. Buragohain, A. Bhunia, C. Janiak and S. Biswas, *CrystEngComm*, 2016, **18**, 7855–7864.

9 S. Dissegna, K. Epp, W. R. Heinz, G. Kieslich and R. A. Fischer, *Adv. Mater.*, 2018, **30**, 1704501.

10 C. Atzori, G. C. Shearer, L. Maschio, B. Civalleri, F. Bonino, C. Lamberti, S. Svelle, K. P. Lillerud and S. Bordiga, *J. Phys. Chem. C*, , DOI:10.1021/acs.jpcc.7b00483.

11 A. Airi, C. Atzori, F. Bonino, A. Damin, S. Øien-ØDegaard, E. Aunan and S. Bordiga, *Dalt. Trans.*, 2019, **49**, 12–16.

12 A. W. Stubbs, L. Braglia, E. Borfecchia, R. J. Meyer, Y. Román-Leshkov, C. Lamberti and M. Dincă, *ACS Catal.*, 2018, **8**, 596–601.

13 S. M. Chavan, G. C. Shearer, S. Svelle, U. Olsbye, F. Bonino, J. Ethiraj, K. P. Lillerud and S. Bordiga, *Inorg. Chem.*, 2014, **53**, 9509–9515.

14 G. C. Shearer, J. G. Vitillo, S. Bordiga, S. Svelle, U. Olsbye and K. P. Lillerud, *Chem. Mater.*, 2016, **28**, 7190–7193.

15 F. Bonino, C. Lamberti, S. M. Chavan, J. G. Vitillo and S. Bordiga, in *Metal Organic Frameworks as Heterogeneous Catalysts*, eds. F. Llabrés i Xamena and J. Gascon, Royal Society of Chemistry, Cambridge, 2013, pp. 76–142.

16 S. Bordiga, F. Bonino, K. P. Lillerud and C. Lamberti, *Chem. Soc. Rev.*, 2010, **39**, 4885–4927.

17 K. A. Lomachenko, J. Jacobsen, A. L. Bugaev, C. Atzori, F. Bonino, S. Bordiga, N. Stock and C. Lamberti, *J. Am. Chem. Soc.*, 2018, **140**, 17379–17383.

18 M. Šimenas, M. Kobalz, M. Mendt, P. Eckold, H. Krautscheid, J. Banys and A. Pöppl, *J. Phys. Chem. C*, 2015, **119**, 4898–4907.

19 B. E. G. Lucier, S. Chen and Y. Huang, *Acc. Chem. Res.*, 2018, **51**, 319–330.

20 M. Lammert, C. Glißmann and N. Stock, *Dalt. Trans.*, 2017, **46**, 2425–2429.

21 L. Valenzano, B. Civalleri, S. Chavan, S. Bordiga, M. H. Nilsen, S. Jakobsen, K. P. Lillerud and C. Lamberti, *Chem. Mater.*, 2011, **23**, 1700–1718.

22 T. Islamoglu, D. Ray, P. Li, M. B. Majewski, I. Akpinar, X. Zhang, C. J. Cramer, L. Gagliardi and O. K. Farha, *Inorg. Chem.*, 2018, **57**, acs.inorgchem.8b01748.

23 J. H. Cavka, S. Jakobsen, U. Olsbye, N. Guillou, C. Lamberti, S. Bordiga and K. P. Lillerud, *J. Am. Chem. Soc.*, 2008, **130**, 13850–13851.

24 R. Dovesi, A. Erba, R. Orlando, C. M. Zicovich-Wilson, B. Civalleri, L. Maschio, M. Rérat, S. Casassa, J. Baima, S. Salustro and B. Kirtman, *Wiley Interdiscip. Rev. Comput. Mol. Sci.*, 2018, **8**, e1360.

25 T. Islamoglu, D. Ray, P. Li, M. B. Majewski, I. Akpinar, X. Zhang, C. J. Cramer, L. Gagliardi and O. K. Farha, *Inorg. Chem.*, 2018, **57**, 13246–13251.

26 F. Nouar, M. I. Breeze, B. C. Campo, A. Vimont, G. Clet, M. Daturi, T. Devic, R. I. Walton and C. Serre, *Chem. Commun.*, 2015, **51**, 14458–14461.

27 F. Bonino, A. Damin, S. Bordiga, C. Lamberti and A. Zecchina, *Langmuir*, 2003, **19**, 2155–2161.

28 K. Chakarova, I. Strauss, M. Mihaylov, N. Drenchev and K. Hadjiivanov, *Microporous Mesoporous Mater.*, 2019, **281**, 110–122.